Article

Integrated Risk Assessment for Robustness Evaluation and Resilience Optimisation of Power Systems after Cascading Failures

Jesus Beyza * and **Jose M. Yusta**

Department of Electrical Engineering, University of Zaragoza, Maria de Luna 3, 50018 Zaragoza, Spain;
jmyusta@unizar.es
* Correspondence: jbeyza@unizar.es

Abstract: Power systems face failures, attacks and natural disasters on a daily basis, making robust-
ness and resilience an important topic. In an electrical network, robustness is a network's ability
to withstand and fully operate under the effects of failures, while resilience is the ability to rapidly
recover from such disruptive events and adapt its structure to mitigate the impact of similar events
in the future. This paper presents an integrated framework for jointly assessing these concepts
using two complementary algorithms. The robustness model, which is based on a cascading failure
algorithm, quantifies the degradation of the power network due to a cascading event, incorporating
the circuit breaker protection mechanisms of the power lines. The resilience model is posed as a
mixed-integer optimisation problem and uses the previous disintegration state to determine both
the optimal dispatch and topology at each restoration stage. To demonstrate the applicability of the
proposed framework, the IEEE 118-bus test network is used as a case study. Analyses of the impact of
variations in both generation and load are provided for 10 simulation scenarios to illustrate different
network operating conditions. The results indicate that a network's recovery could be related to the
overload capacity of the power lines. In other words, a power system with high overload capacity
can withstand higher operational stresses, which is related to increased robustness and a faster
recovery process.

Keywords: cascading failures; power systems security; resilience; restoration; robustness

1. Introduction

Critical infrastructure systems are integral to the everyday activities of modern life. Among these systems, power transmission networks are responsible for reliably and safely meeting power demands at different points in a power system. In daily operation, these networks can experience attacks, failures, natural disasters, etc., all of which can severely degrade the entire function of the infrastructure [1]. The transmission system operator (TSO) must adjust the network topology to increase the power transfer capacity between different areas.

Figure 1 depicts the behaviour of the power system when it is subject to failures or natural disasters. In this figure, the variable t represents the transitions in time between the different phases and P(t) represents variations in the load over time. Note that the sequence consists mainly of five states. In the normal operation state ($t_0 \rightarrow t_{NO}$), the power grid is operating and satisfying the electrical demand safely (P_{NO}) before an unwanted event occurs. Disruption is the phase experienced by the infrastructure immediately after a failure or high-impact, low-probability (HILP) event occurs and is followed by severe degradation of network function ($t_{NO} \rightarrow t_D$). At this point, the load is only partially maintained (P_d). In the preparation stage ($t_D \rightarrow t_{FP}$), the TSO assesses the conditions of the infrastructure and determines which actions must be implemented during the recovery stage ($t_{FP} \rightarrow t_{FR}$). The process ends once the network returns to the load levels that were present before the disruptive event (P_{NO}). This final stage can take hours or even days.
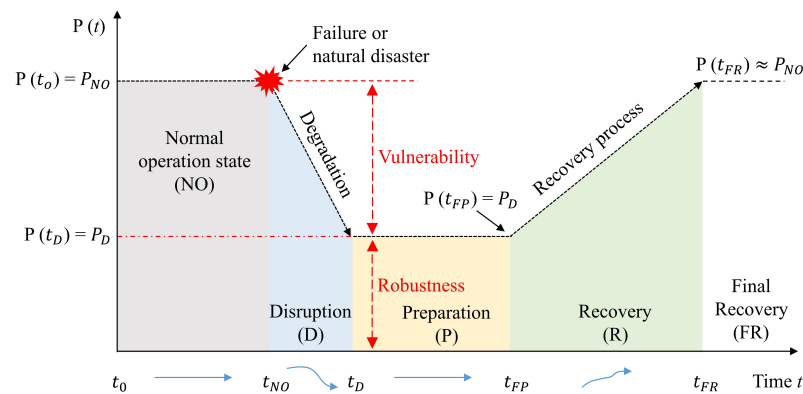
Figure 1. Power system behaviour during failures or natural disasters (representation adapted from [1,2]).

In the field of electrical engineering, robustness studies assess the performance of a network against the loss of multiple assets, while resilience studies analyse the ability of a system to rapidly recover from such disruptive events and adapt its operation and structure to prevent or mitigate the impact of similar events in the future [3,4]. Both concepts are important because they describe the performance of a power system during and after a disturbance or contingency.

Robustness assessment is the most appropriate tool to measure the performance of infrastructure during extreme events, quantify the structural performance of the entire network skeleton and identify the weakest buses that require significant reinforcement [5]. Resilience assessment is the most appropriate tool to analyse the capacity of the system to anticipate, absorb, adapt and recover from such events [6].

Resilience is a novel field of research that requires techniques to solve different problems associated with the protection and recovery of electrical infrastructure. Some researchers have assessed resilience by considering system topology, link switching capabilities and different human-made disaster scenarios [7]. Other researchers have proposed optimal design frameworks to improve resilience and protect the network against extreme weather events such as earthquakes, floods and ice storms [8,9].

Moreover, due to the increasing occurrence of outages and the growing interdependencies between networks, it is vital to understand the resilience of critical infrastructure systems. The most notable existing studies have presented improved approaches to measure resilience and have proposed better decision-making processes for recovery planning after a disruptive event [10–12]. These works have not only identified faster recovery but have also proposed mechanisms to improve the responsiveness of a network.

Other works have considered how renewable resources may be essential to improving the resilience of power systems. In this context, some academics have indicated that the performance of PV systems and hybrid systems composed of wind, PV and batteries can increase operational efficiency and improve reliability and resilience after a natural disaster [13–15].

Similarly, the increase in power outages due to climate deterioration has accelerated research in this area. Several researchers and decision-makers have indicated that more coordinated studies are needed to improve grid resilience and reliability [16]. Other scholars have suggested that optimal restoration strategies that incorporate resilience indicators are also required [17].

Fundamental changes in generation structure and profiles alongside increased demands for robustness and resilience have created the need for new operational and planning practices for modern networks. Cicilio et al. [18] reviewed research that explores the changing generation profile, cutting-edge practices to address resilience and the combination of both topics. Other scholars have offered integrated decision-making analyses

to characterise resilience, robustness, restoration agility and load criticality [19,20]. The objective of this existing work is to evaluate different infrastructure reconfiguration options and select the optimal solution for implementation in both cases.

Resilience also involves a process of detection, anticipation, learning and reconfiguration. In this context, some academics have proposed to reconfigure the power grid using economic model predictive control algorithms [21], deep learning and robust optimisation [22], data-driven batch-constrained reinforcement learning algorithms [23] and Markov decision process models [24].

Smart grid resilience is another relatively young field of research which has not yet been adequately defined. Plotnek and Slay [25] proposed guidelines to orient additional research in this area of study.

The authors of [26–31] provided a comprehensive classification of definitions, metrics, guidelines, practical challenges and technical and practical problems in power system resilience research.

After a contingency or cascading failure, the state of disintegration of the power system is a function of robustness, whereas resilience depends on robustness and the speed of the recovery of the lost load. Most works ignore the initial decay of system conditions, which could be composed of multiple islands and isolated assets. Therefore, new procedures should consider the extent of initial disintegration to improve the recovery process.

This paper postulates that the concepts of robustness and resilience should be integrated within a sequential decision framework to study the impact of disturbances on power systems in detail. Joint analysis of robustness and resilience studies can improve network structural performance, system planning, reliability and even security of supply. A contingency or event in a power network with low robustness can affect the restoration time of isolated assets. In such situations, resilience studies must consider the initial state of disintegration or decay of the infrastructure. The objective of this work is to demonstrate that disintegration plays an important role in the recovery process, as a large number of isolated assets makes it difficult to determine the optimal order in which to reconnect network assets.

Thus, the main purpose of this article is to propose an integrated framework to study both the robustness and resilience of an electrical power system. A system can function under normal operating conditions until one element is lost, triggering adverse effects such as cascading failures that impact a significant portion of the network. Actions are subsequently taken to recover the lost electricity demand in a coordinated manner both in the dispatch of generation and in the optimal reconfiguration of the infrastructure topology.

The robustness described in this work is conducted by running an iterative cascading failure procedure that involves initially removing a link, running direct current power flows, identifying and eliminating overloaded links, quantifying the number of islands and isolated elements and measuring whether demand is satisfied within the network with each iteration of decomposition. On the other hand, the resilience study is a mathematical optimisation problem that considers the optimal redispatch of generation and optimal reconfiguration of the topology. In real-world situations, the TSO makes recovery decisions in sequential time intervals (i.e., the TSO first plans the actions to be taken and, after their execution, analyses the outcome before proceeding to the next restoration steps). In this paper, this sequential decision-making process is improved by formulating it as an optimisation problem to always ensure the best set of redispatch and reconfiguration actions are selected throughout the entire infrastructure recovery process. This formulation should recover maximum demand in the shortest possible time.

However, the latter is a complex mathematical problem with multiple possible decisions at each restoration stage, as the number of possible actions grows exponentially with the number of iterations and has very high computational complexity. The aim of this work is to provide the first solution to this complex problem by developing a procedure to determine which power lines should be closed at each recovery stage. The set of lines identified should not cause overloads on operational links and should maximise the recovered

load on the network. This process would provide operators with complete information to make their decisions after a widespread collapse or blackout.

In short, the proposed sequential framework uses the robustness study to determine the initial state of disintegration of the network and uses this state information as input data for the resilience study. The resilience study is posed as a mixed-integer optimisation problem constructed from the direct current power flow equations, where the integer variables represent the operational state of the power lines (i.e., open or closed). In general terms, the proposed framework calculates optimal generation dispatches and determines the links to be closed for optimal recovery of the network topology. The latter process is limited by the maximum number of lines that can be operated in each iterative step. During the recovery process, active power flows on power lines are considered to avoid overloading other assets.

Notably, this proposal does not address the reactive power limits of the generators or the voltage magnitudes in each of the buses of the electrical network. Instead, the developed procedure could complement other work already published in the scientific literature.

The simulation framework runs on the well-known IEEE 118-bus test system, from which different simulation scenarios are built to demonstrate the scope of the proposed methodology [32]. This network was chosen because it is a sufficiently meshed system and can be applied to many studies with a reasonable solution time but is sufficiently detailed to reflect the real complexities of robustness and resilience studies. This system includes the main generation and transmission facilities, representing a simple and representative model of a real grid. The basic notion is to best illustrate some configurations that can be found in a disintegrated power system. Of course, the simulation framework can be applied and expanded to any other electrical power system.

The rest of the article is organised as follows. Section 2 describes the cascading failure model for determining the initial disintegration state of a power grid. Section 3 details the mathematical model of power system restoration based on a mixed-integer optimisation problem. Section 4 describes the case study and presents the simulation results obtained after applying the two procedures described in the previous sections. Finally, Section 5 draws the main conclusions of this paper and presents some future research directions.

2. Degradation of the Power System

This section presents the procedure developed to assess the robustness of a power system. A cascading failure model, which incorporates models of the protection mechanisms for power lines, is combined with a graph traversal algorithm. The proposed framework accurately captures the state of infrastructure degradation resulting from a failure or HILP event.

Robustness is an internal characteristic of power grids that measures the a system's ability to withstand the effects of faults [33] and is often quantified in terms of the largest connected component, both before and after cascading events [34]. A cascading failure is a sequence of events that begins with one or more disturbances, causing a series of outages in other network components [35]. Cascading can be initiated by multiple factors, such as voltage and frequency instabilities, malfunctioning control devices, human errors, line overloads or deliberate attacks.

To determine the impact of cascading failures, the performance of the network is measured as a function of the connected load after several outages. Here, the satisfied demand (SD) index is used [36,37], and a cascading failure simulation algorithm is proposed.

2.1. Basis of the Cascading Interruption Modelling

The power system can be represented as a graph composed of nodes and links, where the former represent buses, generators and loads, while the latter represent transformers and electric transmission lines (see Figure 2a).
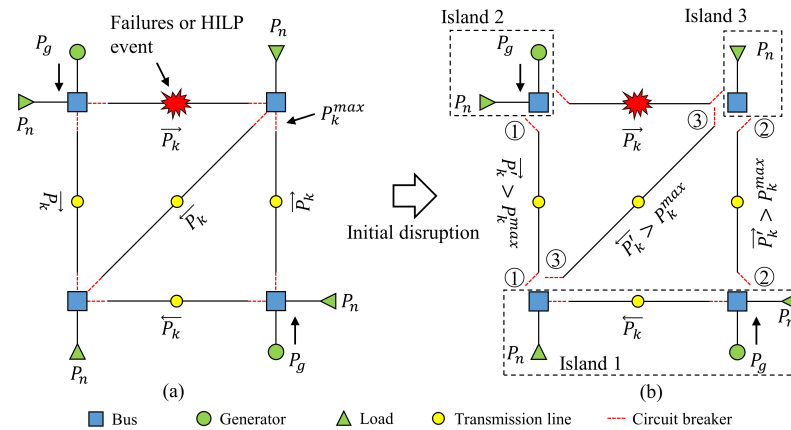
Figure 2. Initial interruption. Operation of power line circuit breakers: (**a**) initial state; and (**b**) first interruption state.

Power flows are a function of Kirchhoff's laws, where the physical parameters of the lines and the voltages and angles of the buses determine the flows within the infrastructure. In this manuscript, the direct current power flow (DCPF) equations are used for simulation purposes [38].

The maximum power transfer capacity (P_k^{max}) of the lines is generally determined using stability constraints, voltage drops and thermal effects. This document assumes that the maximum flow is related to the initial power flow (P_k), as shown in (1), where $\alpha_k > 1$.

$$P_k^{max} = \alpha_k \cdot P_k \quad \forall k \in K \tag{1}$$

Equation (1) models the protection mechanisms of the power lines by introducing a tolerance parameter, α_k. A circuit breaker generally trips when the power flow on the line exceeds an overload threshold. Circuit breakers are assumed to operate when $P_k > P_k^{max}$. Note that the overload tolerance parameter in (1) is defined so that the MVA rating for a power line is not violated.

Cascading failure propagation can lead to the formation of multiple islands, as shown in Figure 2b. In these situations, the load flow problem may not converge, so it is necessary to incorporate a graph traversal algorithm to identify subsets formed in the decomposition stage. The depth-first search (DFS) algorithm is used to solve this problem [39]. This algorithm identifies and sorts the islands each time one or more power lines are disconnected.

2.2. Cascading Failure Algorithm

Algorithm 1, also depicted in the flowchart in Figure 3, defines the proposed procedure for evaluating the disruption stage using the simulation assumptions presented above.

The iterative procedure starts by calculating the power flows and determining the maximum power transfer capacity of the lines with (1). The most loaded power line is then disconnected due to an HILP event, the changes in P_k are determined and the constraint $|P_k| < P_k^{max} \; \forall k \in K$ is verified. If this constraint is not met, the circuit breakers are tripped according to the scheme in Figure 2, and the DFS algorithm immediately monitors the formation of the islands. This technique is used because it is a method for scanning a finite, undirected graph and is widely recognised as a powerful technique for solving various graph problems. The algorithm starts at a root node and scans along each branch before backtracking [39].

Algorithm 1: Disruption stage. Cascading failures.

Input: Technical data of the electrical network and α

Output: Degradation of the power grid. Set of islands I, state of branches μ_k, set of isolated elements E, and satisfied demand SD_s

Step 1. *Initialisation*: $E = \varnothing$ and $SD_{base} = \sum_{d \in D} d$;

Step 2. *Power flows*: calculate $P_k^s \in K$ for all power lines of the infrastructure in stage s; determine P_k^{max} with (1);

Step 3. *Starting point*: eliminate the most loaded power line, k'; set $\mu_{k'} = 0$;

Step 4. *Calculate power flows*: determine the increases or decreases in each $P_k^s \ \forall K$, using DC power flows; set $s = 1$ for the first step;

Step 5. *Trigger mechanisms for circuit breakers*: evaluate the condition $|P_k^s| < P_k^{max} \ \forall K$. If the condition is not met, set $\mu_k^s = 0$ for the triggered power lines k and go to Step 6; otherwise, go to Step 10;

Step 6. *Graph traversal algorithm*: use DFS to determine islands $I = \{I_1, I_2, \ldots, I_N\}$ and isolated elements E;

Step 7. *Energy balance*:
  (a) for each island I_i with generators, $g \in I_i$, evaluate
    - if $\sum_{g \in I_i} P_g < \sum_{d \in I_i} P_d$, set $D_{I_i}^s = \sum_{g \in I_i} P_g$ in stage s;
    - if $\sum_{g \in I_i} P_g > \sum_{d \in I_i} P_d$, set $D_{I_i}^s = \sum_{d \in I_i} P_d$ in stage s;
  (b) for each island I_i without generators, $g \in I_i$; set $D_i^s = 0$ and $E_i = M_i$;

Step 8. *Satisfied demand*: Calculate $SD_s = \frac{\sum_{i \in I} D_{I_i}^s}{SD_{base}}$ for iteration s;

Step 9. *Iterations*: set $s = s + 1$ and go to Step 4;

Step 10. *Termination*: if $|P_k^s| < P_k^{max} \ \forall k$ or $E = M$, the algorithm ends.
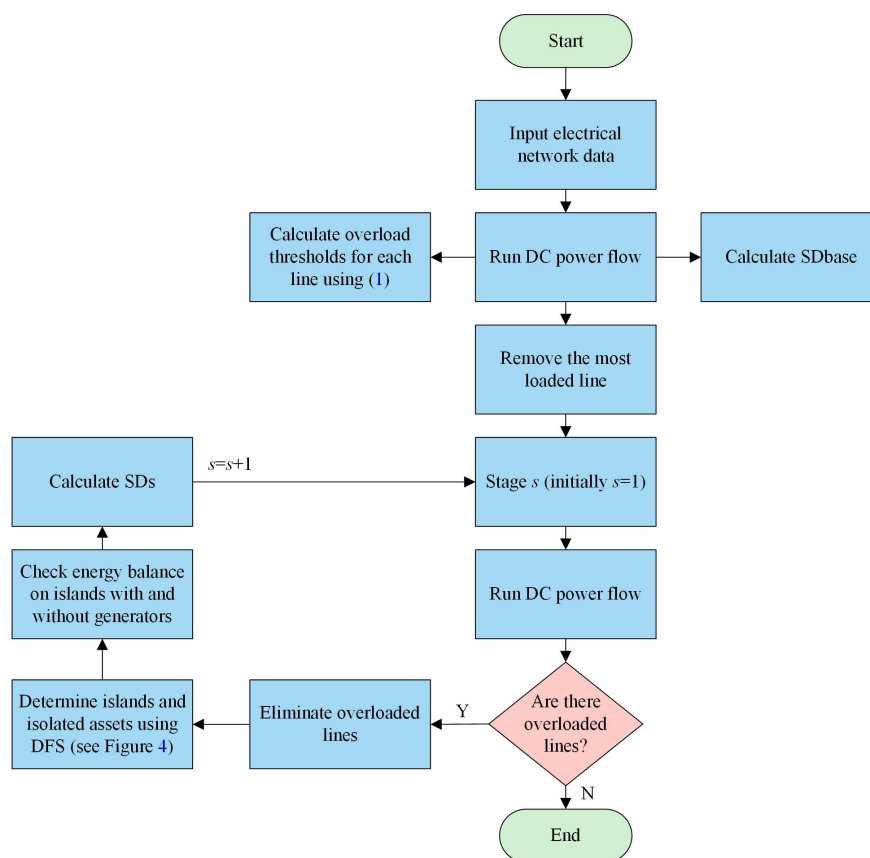

Figure 3. Flowchart of Algorithm 1.

Figure 4 presents the tree structure of the cascading failure process used in Algorithm 1. Here, islands without generation are considered dead and are marked in red, while islands

with generation are marked in green. All intermediate islands where cascading failures continue are marked in blue. The tree structure demonstrates how an island can undergo changes during the cascading failure process (*s*) and disintegrate into several islands, some of which remain operational, and others of which are deeply affected by the disintegration. The cascading failure continues and is repeated on all the intermediate islands marked in blue. The redistribution of the power flows may cause additional overloads on other power lines in the network. Consequently, each intermediate island may result in the formation of different islands, so the procedure continues simultaneously on these new islands.

The SD index used in Algorithm 1 measures the robustness of the power grid by quantifying the SD at each stage of network disintegration. This measure varies between 0 and 1; therefore, as the SD indicator decreases, so does the robustness of the infrastructure.
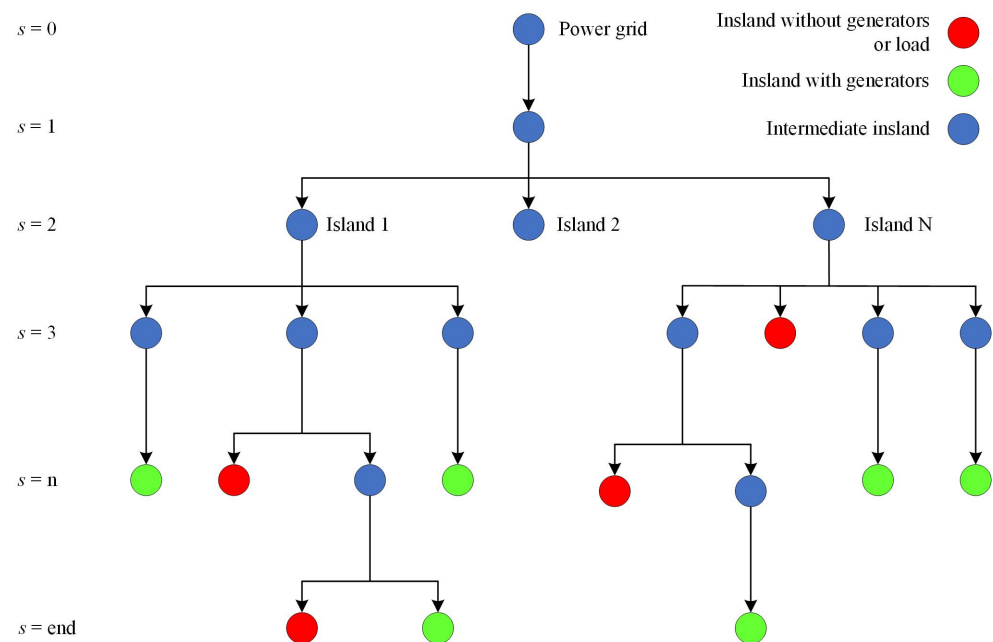

Figure 4. A tree structure of the cascading failure process.

3. Recovery of the Power System

Power system restoration is a highly complex tasks, as the TSO must be prepared with a restoration plan that enables fast and safe recovery of the system. Moreover, the TSO must carefully attend to the energy balance, active and reactive power control, voltage condition and power system stability [40].

Section 3 presents the proposed methodology for recovering a disintegrated electrical network composed of multiple islands and isolated assets. The developed algorithm is based on mixed-integer linear programming and uses the DCPF equations. Here, voltage magnitudes and standing phase angles may not be a major concern, so DCPF studies provide sufficient accuracy in the results, as indicated in [41].

DC Power Flows with Line Drive Incorporation

DCPF is an estimate of power flows in AC power systems. DCPF only considers active power flows and neglects reactive power flows. This method is convergent and non-iterative and is used whenever fast estimates of power flows are required [38]. This formulation is used and power line switching is also incorporated.

The proposed mixed-integer optimisation problem maximises the recovered satisfied demand ($SD_s - SD_{s-1}$) at each step *s*, as shown in Equation (2), by dispatching generation units and reconnecting power lines.

For each step *s*:

$$max\ (SD_s - SD_{s-1}) \tag{2}$$

subject to:

$$P_g^{min} \leq P_g^s \leq P_g^{max} \quad \forall g \in G \tag{3}$$

$$P_k^{min} \cdot \mu_k^s \leq P_k^s \leq P_k^{max} \cdot \mu_k^s \quad \forall k \in K \tag{4}$$

$$\Delta_n^{min} \leq \Delta_n^s \leq \Delta_n^{max} \quad \forall n \tag{5}$$

$$-\sum_{k \in K} P_k^s - \sum_{g \in G} P_g^s - \sum_{d \in D} P_d^s = 0 \quad \forall n \tag{6}$$

$$B_k \cdot (\Delta_n^s - \Delta_m^s) - P_k^s \geq 0 \quad \forall k \tag{7}$$

$$-B_k \cdot (\Delta_n^s - \Delta_m^s) - P_k^s \leq 0 \quad \forall k \tag{8}$$

$$\sum_{k \in K} \mu_k^s \leq N_c \tag{9}$$

$$SD_s = \sum P_n^s \quad \forall n \tag{10}$$

In this formulation, power lines have binary variables μ_k, which represent the switching states of the links (open, $\mu_k = 0$, and closed, $\mu_k = 1$). Moreover, Constraint (9) is included to limit the maximum number of lines to be closed in each recovery iteration.

Constraint (3) limits the power produced by the generators between their maximum and minimum limits; Constraint (4) controls the power passing through the links; Constraint (5) determines the angles of each bus; Constraint (6) incorporates the nodal balance equations; and Constraints (7) and (8) include the Kirchhoff's laws. Finally, Constraint (9) determines the lines operated in each iterative step, as identified by the binary variable $\mu_k^s = \{0, 1\} \forall k \in K$. There is no industry consensus on the maximum number of lines that can be switched during each stage of power grid restoration, as the latter depends on the physical characteristics of the infrastructure and the procedures applied by each control centre.

The output of the optimisation problem consists of the recovered satisfied demand ($SD_s - SD_{s-1}$), the energy produced by the generators (P_g) and the switching states of the power lines (μ_k) for each restoration stage *s*.

Algorithm 2 describes the iterative procedure for determining power system recovery. This algorithm uses the output of Algorithm 1 as its input. Figure 5 presents the flowchart of Algorithm 2.

Algorithm 2: Recovery process. Mixed-integer optimisation problem.

Input: the output of Algorithm 1 (set of islands *I*, state of branches μ_k, set of isolated elements *E* and remaining satisfied demand $SD_{remaining}$) and the number of lines to be reconnected N_c in each step *s*.
Output: SD_s and $\mu_k^s \forall k$ in each recovery step *s*
Step 1. *Inicialisation*: set $SD_s = SD_{remaining}$;
Step 2. *Build the problem*: set the minimum and maximum parameters of the constraints (3)–(5). The thresholds of (4) are initially determined in Algorithm 1;
Step 3. *Solve the mixed-integer optimisation problem*: maximise (2), subject to the constraints in (3)–(10);
Step 4. *Solution*: save the results of SD_s and μ_k^s; set the restored variables μ_k^s as constants μ_k^s=1 for all subsequent stages;
Step 5. *Evaluation*: if $\forall k \in (K-k')$: $\mu_k^s = 1$ and go to Step 7; otherwise, go to Step 6;
Step 6. *Iterations*: set *s* = *s* + 1 and go to Step 3;
Step 7. *Termination*: if $\forall k \in (K-k')$ and $\mu_k^s = 1$; the algorithm ends.
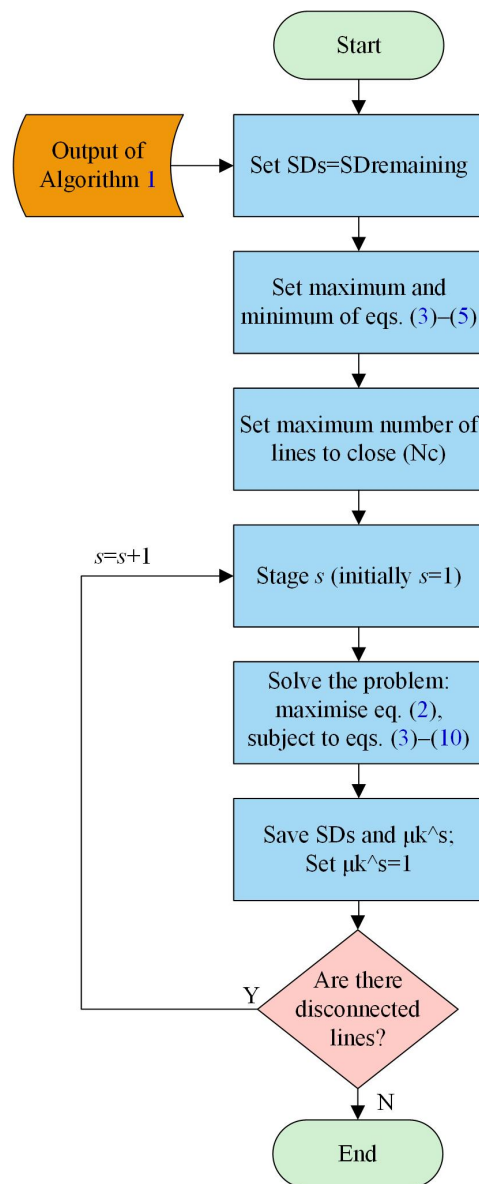

Figure 5. Flowchart of Algorithm 2.

4. Simulation and Results

The simulation results obtained after applying the two developed algorithms to the well-known IEEE 118-bus test network are presented below. Here, costs of generators were not considered, line resistances were ignored and power losses were neglected. Both algorithms were programmed and executed on the MATLAB platform, using a personal computer with an Intel® Core^{TM} i7 3.40 GHz CPU and 32 GB of RAM.

4.1. Normal Operation State: IEEE 118-Bus Test System

This IEEE 118-bus test case represents a simple approximation of the American Electric Power system (in the U.S. Midwest) and contains 54 generators, 186 lines, 14 capacitors and 99 loads. The technical data of the system can be found in [32].

In the normal operation state, the system safely satisfies a load of 4242 MW, and the coupled generators can produce up to 9721 MW. A parameter $\alpha = 1.5$ is applied such that the maximum capacity of the lines is 1.5 times the base flow; therefore, the lines operate at about 70% of their capacity. Moreover, the Δ_n^{min} and Δ_n^{max} for the angles are limited to between -0.6 and -0.6 radians. The P_g^{min} and P_g^{max} for the generators can be found in [38]. Figure 6 depicts this system condition (State A).
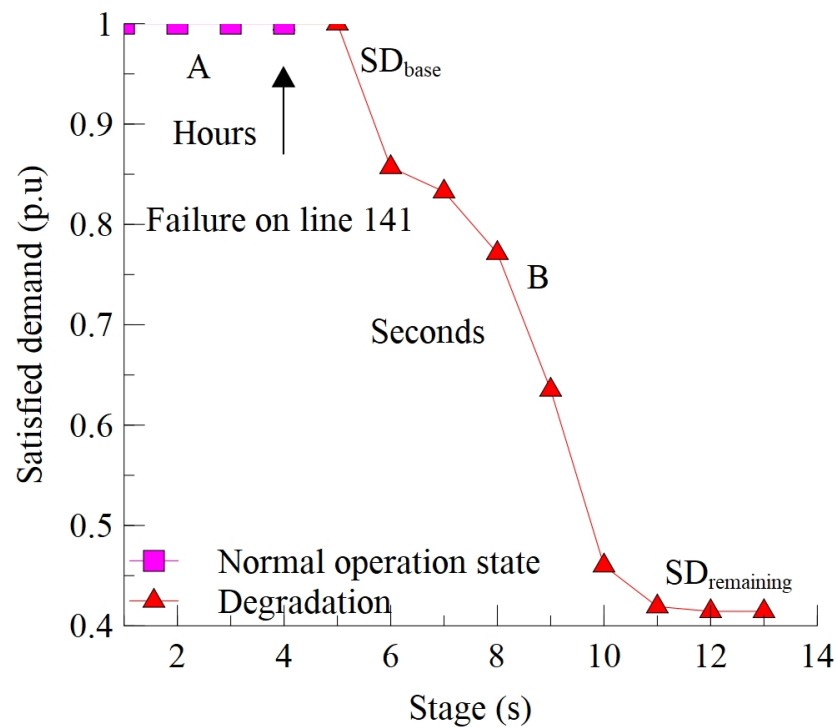
Figure 6. Degradation of the IEEE 118-bus test network. Results obtained using Algorithm 1.

4.2. Disruption State: Degradation of the Power System

Figure 6 plots the degradation of the studied network (State B) due to the non-trivial loss of line 141 (89–92) at stage $s = 4$ ($k' = 141$ and $\mu_{141}' = 0$). As this line was the most loaded line, it was assumed that an HILP event occurred there. The plotted results were obtained after applying Algorithm 1, as described in Section 2.2. The computational time for Algorithm 1 was 0.12 min.

The curve represents the satisfied demand as a function of the cascading stages *s*. When all assets were initially connected, the SD index had a value of 1. Subsequently, the SD index gradually decreased to a value of 0 as the power system disintegrated due to circuit breakers operations. At this point, the infrastructure may have been composed of islands with and without generation and isolated assets.

The results indicate that the IEEE 118-bus test network reached its maximum degradation point at stage $s = 13$, at which point approximately 40% of the load remained connected. Likewise, the damage caused by the loss of link 141 caused the system to disintegrate into 15 islands. Here, four islands had a load of 1092 MW. In parallel, these four islands had a load shedding of 196 MW to satisfy the conditions of balance between generation and load (666 MW). Similarly, seven islands with a load of 1000 MW were inoperative, and 71 lines were open due to overloading. There were 44 isolated buses with a total load of 1288 MW. Figure 7 presents the topology of the IEEE 118-bus test network and the various islands in the system.
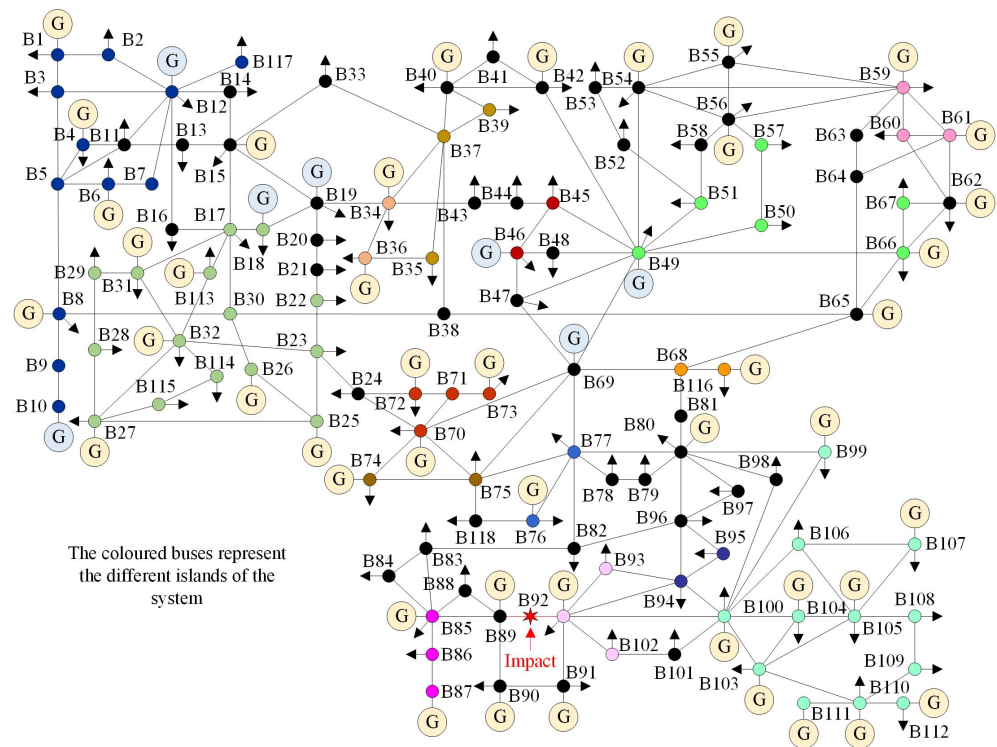
Figure 7. Schematic representation of the power system under study after the cascading failures took place.

The above results were obtained by applying a tolerance parameter $\alpha = 1.5$. Depending on this value, different degradation states of the electrical network can be obtained due to line overloads. For example, Figure 8 presents the final SD for different values of alpha between $\alpha = 1$ and $\alpha = 2$. Note that, as the overload parameter α increases, the satisfied demand also increases. Thus, the recovery process is related to the overload capacity of the power lines, as infrastructure with high overload capability can withstand higher operational efforts, which is related to less degradation and, consequently, to a faster recovery process.
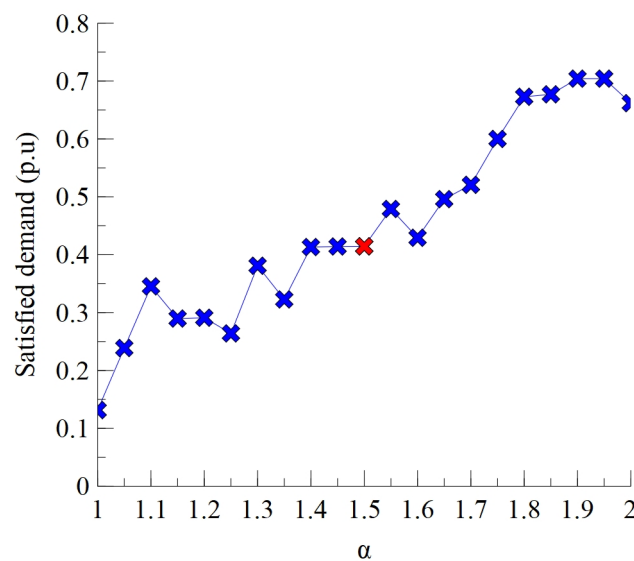

Figure 8. Overload tolerance parameter.

On the contrary, an electrical infrastructure with low overload capability achieves lower SD percentages at the end of the degradation process, which is related to a slower recovery process. A tolerance parameter $\alpha = 1.5$ was chosen in this paper because it is an acceptable intermediate value for the case studies, as indicated in Figure 8.

4.3. Preparation State

In this phase, the TSO analyses the state of the network after the cascading failure and prepares the necessary actions or manoeuvres to quickly and safely recover the load and reconnect the isolated assets.

In the engineering field, the TSO could prioritise the reconnection of some loads or some generators or utilise all infrastructure facilities [42–45]. Certain assets may not be available if they have suffered irreversible damage. The TSO carefully evaluates and uses all available resources to quickly restore the network.

In this case study, the disintegrated power grid consisted of 15 islands, 71 open lines, 44 isolated buses and a disconnected load of more than 2000 MW. Three stages were considered to plan recovery actions ($s = 14$ to $s = 16$).

4.4. Recovery Process

The aim of the recovery process is to develop a methodology to restore the operating conditions of the electrical infrastructure after a major disruption. This recovery must comply with several security parameters to avoid further line outages. Algorithm 2 can be applied to determine the optimal recovery of the network under study.

To obtain different recovery plans, the maximum number of lines N_c to be closed at each restoration stage is limited. In this case, values of $N_c = 1, 3, 5$ and 7 were considered. One or seven lines were closed for simulation purposes only; closing three or five lines corresponds to the usual number of safe manoeuvres performed by the TSO. Moreover, line 89–92 could not be reconnected during the recovery process because it was badly damaged.

Figure 9 displays the recovery curves for the different plans obtained using Algorithm 2. Unlike Figure 6, in this case, higher SD values indicate a greater recovered load.
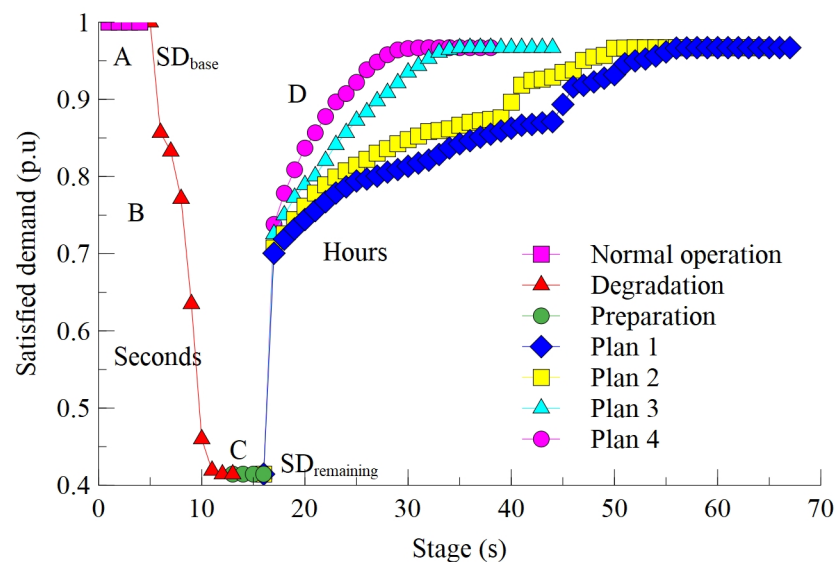

Figure 9. Recovery curves for the IEEE 118-bus test system.

The developed methodology found the optimal solution at each stage to recover the disconnected loads and reconnect the islands and isolated buses. The plans restored the operational network conditions fairly quickly. In the proposed system, manoeuvres are managed in minutes, so the actions that could be taken during this simulation were limited. For example, only one line was reconnected, and the corresponding generation redispatch

was performed with $N_c = 1$. The next action was then executed, and the procedure was repeated. However, recovery would be faster if more manoeuvres could be performed at each interval.

Table 1 reports the different recovery plans according to the number of lines reconnected in each iteration. For illustration purposes, only the lines corresponding to the first recovery iteration are shown (i.e., $s = 17$). The values of recovered load, satisfied demand and computation times are included for each plan.

Table 1. Optimal recovery plans obtained using Algorithm 2 in stage $s = 17$.

Plan	Number of Lines to Be Closed (N_c)	Closed Lines (L)	Recovered Load (MW)	Satisfied Demand (SD_s)	Computation Times (min)
State C				0.414	
1	1	18	1214	0.701	7.357
2	3	18, 63, 80	1243	0.707	37.085
3	5	16, 18, 63, 64, 80	1320	0.726	67.619
4	7	16, 18, 63, 64, 80, 91, 114	1373	0.738	71.649

The first manoeuvre resulted in values of satisfied demand that were similar across the different recovery plans. However, the topological configuration was not the same in each case; therefore, generation redispatch influenced the recovery of isolated loads. Additionally, the calculation time increased with the number of lines to be reconnected because more combinations had to be considered to find the optimal solution.

Recovery was slow when a power line was reconnected (Plan 1), but the system quickly recovered the load and the meshed structure of the network when three power lines were reconnected (Plan 2).

The outcomes of Plans 3 and 4 were almost similar, as were the outcomes of Plans 1 and 2. However, Plans 3 and 4, which involved the reconnection of five and seven lines, respectively, offered better results than Plans 1 and 2. Some topological configurations are evidently better for network meshing since line constraints influence the recovered load. For example, as shown in Figure 9, if the TSO were to follow Plan 3 in the order indicated, 29 stages would be sufficient to recover almost 100% of the load and bring all lines into operation. However, if Plan 1 or 2 was followed, approximately 50 stages would be required.

Table 2 presents the Energy Not Supplied (ENS) results for each recovery plan. The ENS metric is quantified by measuring the area above the recovery curves and considering time intervals of 15 min for each stage s and 20 h of repair time for line 89–92. As the ENS decreases, the recovery plan becomes more efficient. Considering these times and the number of stages, an average time to restore the infrastructure can be obtained. For example, Plan 4 required 23 stages, that is, 5.75 h plus an additional 20 h to repair power line 89–92. In contrast, the proposed study framework obtained the complete solution in approximately 1.2 h (Table 1), so each set of lines computed per iteration required about three minutes. The results can therefore be obtained in parallel to the execution of the corresponding manoeuvres, with an additional 12-min reserve. Of course, other factors that could influence the speed of the recovery of the power system must be considered; however, the times between switching, redispatching and repairing the damaged line correspond to values close to reality. In short, the proposed procedure determined the required manoeuvres before their execution. The TSO could consequently analyse the results and determine the most appropriate and accurate actions, which would guarantee the highest load recovery and the best-operating conditions of the system.

Table 2. Energy Not Supplied for each recovery plan.

Plan	Number of Stages s	Energy not Supplied (MWh)
Base network		0
1	52	135.65
2	49	114.56
3	29	77.06
4	23	63.71

4.5. Variations in Generation and Load

To test the usefulness of the developed algorithms under various generation and load conditions, 10 simulation scenarios were additionally applied, using $\alpha = 1.5$ and $N_c = 5$ as parameters during each recovery stage. Five lines were chosen for this analysis (Plan 3) because five lines is a safer switching number than seven lines (Plan 4) for the considered time interval of 15 min.

Table 3 summarises each of the scenarios studied in this analysis. In the case of generation variation, Scenario G_{89} evaluated the system's degradation and recovery without Generator 89. Scenario G_{89+80} corresponds to the same system, but without Generators 89 and 80. The rest of the scenarios followed the same scheme as above, eliminating the generators with the highest capabilities in descending order. Meanwhile, in the case of load variation, Scenario $L_{+5\%}$ evaluated the system's degradation and recovery with a 5% load increase, while Scenario $L_{+10\%}$ evaluated the system's performance with a 10% load increase. This process was repeated successively for subsequent scenarios until the load increased reached 25%.

Table 3. Study scenarios.

Variation	Scenarios
Generation	$G_{89} \rightarrow G_{89+80} \rightarrow G_{89+80+69} \rightarrow G_{89+80+69+10} \rightarrow G_{89+80+69+10+66}$
Load	$L_{+5\%} \rightarrow L_{+10\%} \rightarrow L_{+15\%} \rightarrow L_{+20\%} \rightarrow L_{+25\%}$

Figure 10 indicates that the base case maintained a satisfied demand of more than 40% after the cascading event. In the rest of the cases analysed with variations in generation and load, the networks collapsed more significantly. The 10 scenarios studied had worse performance than the base case, as the curves always went below in both degradation and recovery. These scenarios show that the IEEE 118-bus test system in its base case is more robust than when it has less generation or more load.

Similar robustness values were obtained in the generation and load scenarios. For example, the satisfied demand after the system degradation process was close to 20% for both the lowest generation scenario ($G_{89+80+69+10+66}$) and the highest load scenario ($L_{+25\%}$).

The curves in Figures 9 and 10 demonstrate that the developed study framework provides optimal recovery strategies for collapsed networks composed of multiple islands and isolated elements. The results also indicate that generation availability conditions could severely affect cascading failures propagation and electrical network recovery.

The conducted simulations demonstrate that the developed procedures can be applied to different operating conditions and disintegration states of power systems. Although the procedures are applied to scenarios of variation in generation and demand, the robustness and resilience models could be combined with other proposals to extend the results presented here.
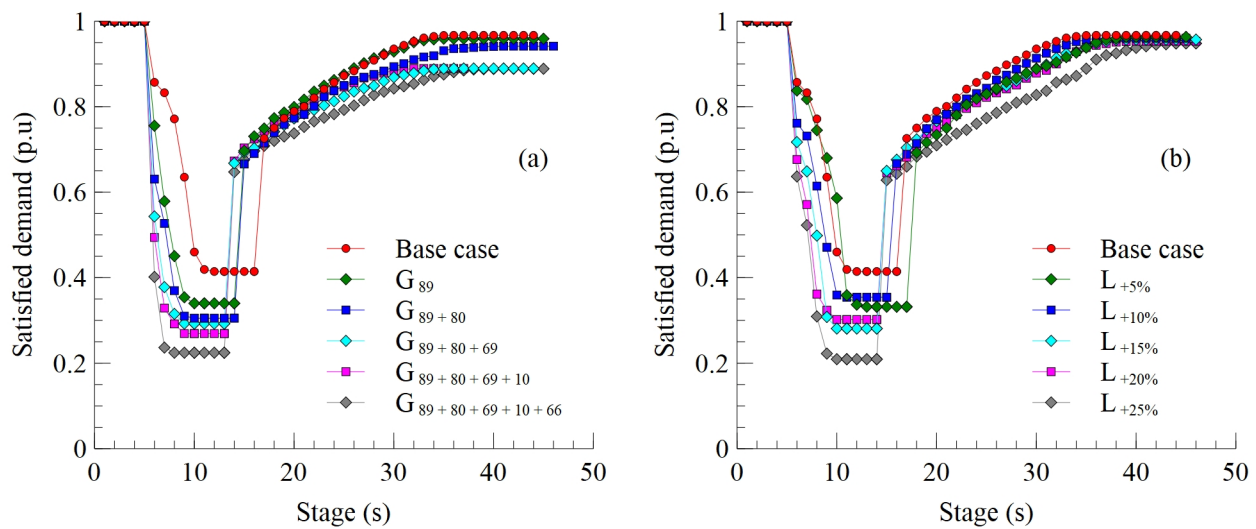
Figure 10. Process of disintegration and recovery of the IEEE-118 bus test system with variations in: (**a**) generation; and (**b**) load.

5. Conclusions

This paper proposes a joint framework for assessing both the robustness and resilience of electric power systems. A cascading failure procedure id used to determine the state of disintegration of a power grid and a mixed-integer optimisation problem id applied to identify the optimal dispatch and topology during the network recovery process. The cascading failure procedure considers the dynamic disintegration of the infrastructure due to the tripping of the circuit breakers of the power lines. The restoration procedure determines the level of generation and the power lines to be closed or opened at each stage of system recovery. In both cases, the satisfied demand index is measured to quantify the power supply within the infrastructure.

The effectiveness and applicability of the proposed framework, which aims to quantify robustness and resilience, was verified using the IEEE 118-bus test system. This paper provides a detailed discussion of the numerical results, demonstrating the efficacy of the proposed procedures and their benefit to end-users and utilities. The TSO could apply different strategies or plans to recover a disconnected load after a high impact event, depending on the switching actions taken.

Renewable energies are becoming increasingly important in the current energy transition scenario of power systems. This considerable increase in renewable generation could affect the performance of a network in the case of a high-impact, low-probability event. Thus, future research and development efforts should explore computationally efficient mathematical methodologies to assess the robustness and resilience of power systems with a high share of renewable energy. The random nature of renewable energies necessitates stochastic models to analyse different operating conditions of a power grid. The resulting models should integrate both indicators and provide solutions for transmission system planners and operators.

Author Contributions: Methodology, J.B. and J.M.Y.; investigation, J.B. and J.M.Y.; validation, J.B. and J.M.Y.; writing—original draft preparation, J.B.; and writing—review and editing, J.B. and J.M.Y. All authors have read and agreed to the published version of the manuscript.

Institutional Review Board Statement: Not applicable.

Informed Consent Statement: Not applicable.

Abbreviations

The following abbreviations are used in this manuscript:

Indices

n,m	Nodes or buses
k	Lines
g	Generators
d	Loads
j	Number of closed power lines
i	Islands
s	Steps

Variables

Δ_n	Voltage angle at node n (radians)
P_k, P_g, P_n	Power flow through line k, generator g, and power demand at node n
μ_k	Binary variable indicating the open or closed state of the power line (open, $\mu_k = 0$, closed, $\mu_k = 1$)
D_i	Demand on each island i
SD_s	Satisfied demand in step s (MW)

Parameters

P_k^{max}, P_k^{min}	Maximum and minimum capacity of the power line k (MW)
P_g^{max}, P_g^{min}	Maximum and minimum capacity of the generator g (MW)
$\Delta_n^{max}, \Delta_n^{min}$	Maximum and minimum voltage angle at node n (radians)
B_k	Susceptance of the power line k
N_c	Maximum number of power lines to be closed at each step s
α_k	Overload tolerance parameter of the power line k

Sets

D	System loads
E	Isolated assets
G	Generators
I	Islands
K	Power lines
L	Closed power lines
M	Nodes or buses

References

1. Jamborsalamati, P.; Moghimi, M.; Hossain, M.; Taghizadeh, S.; Lu, J.; Konstantinou, G. A framework for evaluation of power grid resilience case study: 2016 South Australian blackout. In Proceedings of the 2018 IEEE International Conference on Environment and Electrical Engineering and 2018 IEEE Industrial and Commercial Power Systems Europe (EEEIC/I&CPS Europe), Palermo, Italy, 12–15 June 2018; pp. 1–6.
2. Dehghanian, P.; Aslan, S.; Dehghanian, P. Maintaining electric system safety through an enhanced network resilience. *IEEE Trans. Ind. Appl.* **2018**, *54*, 4927–4937. [CrossRef]
3. Chen, Q.; McCalley, J.D. Identifying high risk Nk contingencies for online security assessment. *IEEE Trans. Power Syst.* **2005**, *20*, 823–834. [CrossRef]
4. Noebels, M.; Preece, R.; Panteli, M. AC Cascading Failure Model for Resilience Analysis in Power Networks. *IEEE Syst. J.* **2020**, 1–12. [CrossRef]
5. Sabouhi, H.; Doroudi, A.; Fotuhi-Firuzabad, M.; Bashiri, M. A novel matrix based systematic approach for vulnerability assessment. *COMPEL Int. J. Comput. Math. Electr. Electron. Eng.* **2020**, *40*, 1–17. [CrossRef]

6.　Stankovic, A. *The Definition and Quantification of Resilience*; IEEE PES Industry Technical Support Task Force: Piscataway, NJ, USA, 2018; pp. 1–4.

7.　Tapia, T.; Lorca, Á.; Olivares, D.; Negrete-Pincetic, M.; Lamadrid L, A.J. A Robust Decision-Support Method Based on Optimization and Simulation for Wildfire Resilience in Highly Renewable Power Systems. *Eur. J. Oper. Res.* **2021**, 1–11. [CrossRef]

8.　Shahbazi, A.; Aghaei, J.; Pirouzi, S.; Niknam, T.; Shafie-khah, M.; Catal ao, J.P. Effects of resilience-oriented design on distribution networks operation planning. *Electr. Power Syst. Res.* **2021**, *191*, 106902. [CrossRef]

9.　Zhao, N.; Yu, X.; Hou, K.; Liu, X.; Mu, Y.; Jia, H.; Wang, H.; Wang, H. Full-time scale resilience enhancement framework for power transmission system under ice disasters. *Int. J. Electr. Power Energy Syst.* **2021**, *126*, 106609. [CrossRef]

10.　Zobel, C.W.; MacKenzie, C.A.; Baghersad, M.; Li, Y. Establishing a frame of reference for measuring disaster resilience. *Decis. Support Syst.* **2021**, *140*, 113406. [CrossRef]

11.　Almoghathawi, Y.; González, A.D.; Barker, K. Exploring Recovery Strategies for Optimal Interdependent Infrastructure Network Resilience. *Netw. Spat. Econ.* **2021**, *21*, 229–260. [CrossRef]

12.　Senkel, A.; Bode, C.; Schmitz, G. Quantification of the resilience of integrated energy systems using dynamic simulation. *Reliab. Eng. Syst. Saf.* **2021**, *209*, 107447. [CrossRef]

13.　Bai, X.; Liang, L.; Zhu, X. Improved Markov-chain-based ultra-short-term PV forecasting method for enhancing power system resilience. *J. Eng.* **2021**, *2021*, 114–124. [CrossRef]

14.　Tawfiq, A.A.; Osama abed el Raouf, M.; Mosaad, M.I.; El-Gawad, A.A.; Farahat, M.A. Optimal reliability study of grid-connected PV systems using Evolutionary Computing Techniques. *IEEE Access* **2021**, *9*, 42125–42139. [CrossRef]

15.　Samy, M.M.; Mosaad, M.I.; El-Naggar, M.F.; Barakat, S. Reliability Support of Undependable Grid Using Green Energy Systems: Economic Study. *IEEE Access* **2020**, *9*, 14528–14539. [CrossRef]

16.　Hossain, E.; Roy, S.; Mohammad, N.; Nawar, N.; Dipta, D.R. Metrics and enhancement strategies for grid resilience and reliability during natural disasters. *Appl. Energy* **2021**, *290*, 116709. [CrossRef]

17.　Yu, Z.; Li, Z.; Qian, T.; Huang, K.; Chen, X.; Tang, W. Optimal Restoration Strategy Based on Resilience Improvement for Power Transmission Systems Under Extreme Weather Events. In Proceedings of the 2020 International Conference on Smart Grid and Energy Engineering, Guilin, China, 13–15 November 2021; IOP Publishing: Bristol, UK, 2021, Volume 645, pp. 1–8.

18.　Cicilio, P.; Glennon, D.; Mate, A.; Barnes, A.; Chalishazar, V.; Cotilla-Sanchez, E.; Vaagensmith, B.; Gentle, J.; Rieger, C.; Wies, R.; et al. Resilience in an Evolving Electrical Grid. *Energies* **2021**, *14*, 694. [CrossRef]

19.　Jamborsalamati, P.; Garmabdari, R.; Hossain, J.; Lu, J.; Dehghanian, P. Planning for resilience in power distribution networks: A multi-objective decision support. *IET Smart Grid* **2021**, *4*, 45–60. [CrossRef]

20.　Tari, A.N.; Sepasian, M.S.; Kenari, M.T. Resilience assessment and improvement of distribution networks against extreme weather events. *Int. J. Electr. Power Energy Syst.* **2021**, *125*, 106414.

21.　Liberati, F.; Di Giorgio, A.; Giuseppi, A.; Pietrabissa, A.; Priscoli, F.D. Efficient and risk-aware control of electricity distribution grids. *IEEE Syst. J.* **2020**, *14*, 3586–3597. [CrossRef]

22.　Zheng, W.; Huang, W.; Hill, D.J. A deep learning-based general robust method for network reconfiguration in three-phase unbalanced active distribution networks. *Int. J. Electr. Power Energy Syst.* **2020**, *120*, 105982. [CrossRef]

23.　Gao, Y.; Wang, W.; Shi, J.; Yu, N. Batch-constrained reinforcement learning for dynamic distribution network reconfiguration. *IEEE Trans. Smart Grid* **2020**, *11*, 5357–5369. [CrossRef]

24.　Wang, C.; Lei, S.; Ju, P.; Chen, C.; Peng, C.; Hou, Y. MDP-based distribution network reconfiguration with renewable distributed generation: Approximate dynamic programming approach. *IEEE Trans. Smart Grid* **2020**, *11*, 3620–3631. [CrossRef]

25.　Plotnek, J.J.; Slay, J. Power systems resilience: Definition and taxonomy with a view towards metrics. *Int. J. Crit. Infrastruct. Prot.* **2021**, *33*, 100411. [CrossRef]

26.　Mahzarnia, M.; Moghaddam, M.P.; Baboli, P.T.; Siano, P. A review of the measures to enhance power systems resilience. *IEEE Syst. J.* **2020**, *14*, 4059–4070. [CrossRef]

27.　Naghshbandi, S.N.; Varga, L.; Purvis, A.; Mcwilliam, R.; Minisci, E.; Vasile, M.; Troffaes, M.; Sedighi, T.; Guo, W.; Manley, E.; et al. A review of methods to study resilience of complex engineering and engineered systems. *IEEE Access* **2020**, *8*, 87775–87799. [CrossRef]

28.　Mishra, D.K.; Ghadi, M.J.; Azizivahed, A.; Li, L.; Zhang, J. A review on resilience studies in active distribution systems. *Renew. Sustain. Energy Rev.* **2021**, *135*, 110201. [CrossRef]

29.　Cheng, Y.; Elsayed, E.; Chen, X. Random Multi Hazard Resilience Modeling of Engineered Systems and Critical Infrastructure. *Reliab. Eng. Syst. Saf.* **2021**, *209*, 107453. [CrossRef]

30.　Aziz, T.; Lin, Z.; Waseem, M.; Liu, S. Review on optimization methodologies in transmission network reconfiguration of power systems for grid resilience. *Int. Trans. Electr. Energy Syst.* **2021**, *31*, 1–38. [CrossRef]

31.　Cantelmi, R.; Di Gravio, G.; Patriarca, R. Reviewing qualitative research approaches in the context of critical infrastructure resilience. *Environ. Syst. Decis.* **2021**, 1–36. [CrossRef]

32.　IEEE. IEEE 118-Bus System. Available online: https://electricgrids.engr.tamu.edu/electric-grid-test-cases/ieee-118-bus-system/ (accessed on 6 April 2021).

33.　Kröger, W.; Zio, E. *Vulnerable Systems*; Springer: London, UK, 2011; p. XIV-204.

34.　Albert, R.; Barabási, A.L. Statistical mechanics of complex networks. *Rev. Mod. Phys.* **2002**, *74*, 1–54. [CrossRef]

35. Vaiman, M.; Bell, K.; Chen, Y.; Chowdhury, B.; Dobson, I.; Hines, P.; Papic, M.; Miller, S.; Zhang, P. Risk assessment of cascading outages: Methodologies and challenges. *IEEE Trans. Power Syst.* **2012**, *27*, 631–641. [CrossRef]

36. Bier, V.M.; Gratz, E.R.; Haphuriwat, N.J.; Magua, W.; Wierzbicki, K.R. Methodology for identifying near-optimal interdiction strategies for a power transmission system. *Reliab. Eng. Syst. Saf.* **2007**, *92*, 1155–1161. [CrossRef]

37. Haidar, A.M.; Mohamed, A.; Hussain, A. Vulnerability assessment of a large sized power system considering a new index based on power system loss. *Eur. J. Sci. Res.* **2007**, *17*, 61–72.

38. Zimmerman, R.D.; Murillo-Sánchez, C.E.; Thomas, R.J. MATPOWER: Steady-state operations, planning, and analysis tools for power systems research and education. *IEEE Trans. Power Syst.* **2010**, *26*, 12–19. [CrossRef]

39. Even, S. *Graph Algorithms*; Cambridge University Press: Cambridge, UK, 2011; pp. 1–189.

40. Martins, N.; de Oliveira, E.J.; Moreira, W.C.; Pereira, J.L.R.; Fontoura, R.M. Redispatch to reduce rotor shaft impacts upon transmission loop closure. *IEEE Trans. Power Syst.* **2008**, *23*, 592–600. [CrossRef]

41. Wood, A.J.; Wollenberg, B.F.; Sheblé, G.B. *Power Generation, Operation, and Control*; John Wiley & Sons: Hoboken, NJ, USA, 2013; pp. 1–656.

42. Panteli, M.; Trakas, D.N.; Mancarella, P.; Hatziargyriou, N.D. Power systems resilience assessment: Hardening and smart operational enhancement strategies. *Proc. IEEE* **2017**, *105*, 1202–1213. [CrossRef]

43. Bie, Z.; Lin, Y.; Li, G.; Li, F. Battling the extreme: A study on the power system resilience. *Proc. IEEE* **2017**, *105*, 1253–1266. [CrossRef]

44. Chanda, S.; Srivastava, A.K. Quantifying resiliency of smart power distribution systems with distributed energy resources. In Proceedings of the 2015 IEEE 24th International Symposium on Industrial Electronics (ISIE), Buzios, Brazil, 3–5 June 2015; pp. 1–6.

45. Panteli, M.; Mancarella, P. Influence of extreme weather and climate change on the resilience of power systems: Impacts and possible mitigation strategies. *Electr. Power Syst. Res.* **2015**, *127*, 259–270. [CrossRef]